JTTEE5 13:66-75
DOI: 10.1361/10599630418167
1059-9630/$19.00 © ASM International

Peer Reviewed

# Improved Oxidation Life of Segmented Plasma Sprayed 8YSZ Thermal Barrier Coatings

*James L. Smialek*

*(Submitted 15 August 2003; in revised form 15 October 2003)*

**Unconventional plasma sprayed thermal barrier coating (TBC) systems were produced and evaluated by interrupted or cyclic furnace oxidation life testing. First, approximately 250 μm thick 8YSZ coatings were directly sprayed onto grit blasted surfaces of PWA 1484, without a bond coat, to take advantage of the excellent oxidation resistance of this superalloy. For nominal sulfur (S) contents of 1 ppmw, total coating separation took place at relatively short times (200 h at 1100 °C). Reductions in the S content, by melt desulfurization commercially (0.3 ppmw) or by hydrogen ($H_2$) annealing in the laboratory (0.01 ppmw), improved scale adhesion and extended life appreciably, by factors of 5-10. However, edge-initiated failure persisted, producing massive delamination as one sheet of coating. Secondly, surfaces of melt desulfurized PWA 1484 were machined with a grid of grooves or ribs (~250 μm wide and high), resulting in a segmented TBC surface macrostructure, for the purpose of subverting this failure mechanism. In this case, failure occurred only as independent, single-segment events. For grooved samples, 1100 °C segment life was extended to ~1000 h for 5 mm wide segments, with no failure observed out to 2000 h for segments ≤2.5 mm wide. Ribbed samples were even more durable, and segments ≤6 mm remained intact for 2000 h. Larger segments failed by buckling at times inversely related to the segment width and decreased by oxidation effects at higher temperatures. This critical buckling size was consistent with that predicted for elastic buckling of a TBC plate subject to thermal expansion mismatch stresses. Thus, low S substrates demonstrate appreciable coating lives without a bond coat, while rib segmenting extends life considerably.**

**Keywords** low sulfur superalloys, no bond coat, oxidation, segmented thermal barrier coating

## 1. Introduction

Conventional air plasma sprayed (APS) and physical vapor deposited (PVD) 8 yttria-stabilized-zirconia (YSZ) thermal barrier coatings (TBCs) are applied to oxidation resistant Ni(Pt)Al or Ni(Co)CrAlY bond coats. Bond coats are needed to prevent premature coating failure by excessive stresses arising from nonprotective scale growth and by interfacial separation due to scale spallation. Successful TBCs have been demonstrated for oxidation resistant substrates without a bond coat, such as for the intermetallic compound NiAl(Zr).[1] Also, since second-generation single-crystal superalloys also exhibit exceptional oxidation resistance, it has been proposed that they are candidates for no bond coat TBCs.[2] Both systems rely on slow-growing healing layers of $\alpha$-$Al_2O_3$. A potential advantage of the no bond coat system is the elimination of deleterious effects associated with creep of a plastic bond coat. Creep effects include raising the stress-free temperature during exposure above the deposition temperature[3] and wrinkling (ratcheting) of aluminide coatings, which produces stress concentrations that initiate cracks.[4]

Good adhesion is imparted by reactive element doping or desulfurization. Reactive element additions are thought to improve scale adhesion by their strong thermodynamic affinity for sulfur (S) and their ability to prevent deleterious S segregation effects on interfacial toughness.[5] Alternatively, scale adhesion may be improved by removing S, either by hydrogen ($H_2$) annealing or melt fluxing. A quantitative correlation between scale adhesion and S and a literature survey can be found in recent reviews,[6,7] with specific attention to low S superalloys.[8-10]

Many of the above precepts may be applied to the cyclic oxidation behavior of TBCs and their delamination failure. By eliminating the bond coat in the current study, the excellent cyclic oxidation resistance of single crystal superalloys was relied upon. This allowed for a direct demonstration of the effects of substrate chemistry on TBC life, although it may not be totally applicable to current real systems using bond coats. The direct effect of bond coat chemistry and the indirect effect of substrate chemistry have been demonstrated for NiAl bond coats and electron beam physical vapor deposition (EB-PVD) YSZ systems.[11-14] Thus one purpose of this paper is to show the dependence of plasma sprayed TBC life on substrate S content. Preliminary results in this regard have been presented previously.[8,15] Another purpose is to use physical barriers to disrupt TBC delamination. These have been introduced as grooves or ribs in the substrate, prior to grit blasting and plasma spraying, as embodied in a recent patent.[16]

## 2. Experimental Procedure

Oxidation coupons of PWA 1484 single-crystal superalloys (nominally Ni-5Cr-5.6Al-10Co-2Mo-6W-9Ta-3Re-0.1Hf by weight) were machined to approximately 0.13 × 1.3 × 1.9 cm rectangles and 0.1 × 2.54 cm diameter disks and polished to a 600 grit finish. Substrates for coating were grit-blasted with 60 grit alumina. Some samples were $H_2$ annealed in a gettered 5%$H_2$/Ar

**James L. Smialek,** NASA Glenn Research Center, 21000 Brookpark Rd., MS 106, Cleveland, OH 44135. Contact e-mail: James.L.Smialek@grc.nasa.gov.

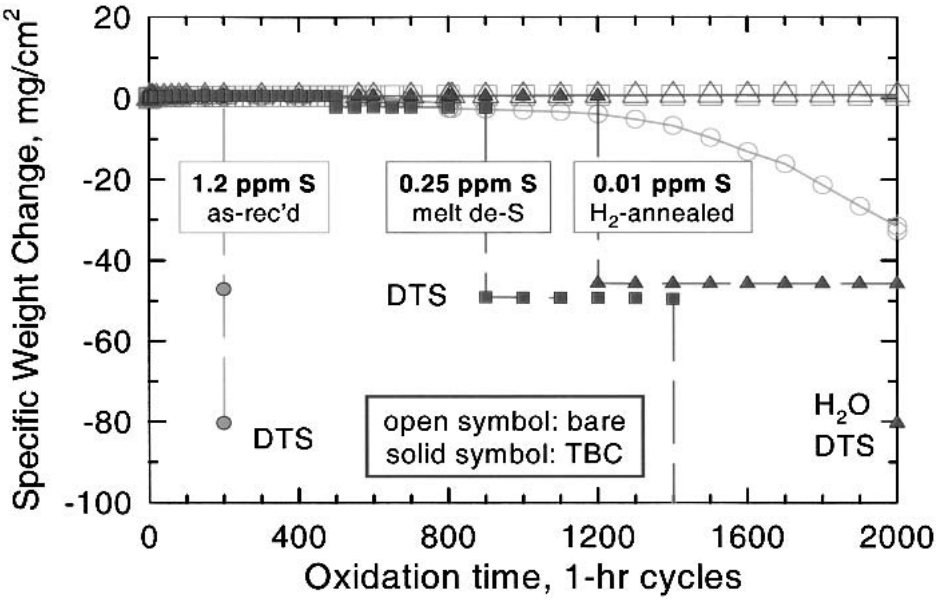


**Fig. 1** Effect of $H_2$-annealing and melt desulfurization on the 1100 °C cyclic oxidation of PWA 1484. Solid lines: bare; dashed lines: coated with 250 μm PS-8YSZ TBC.

flowing gas mixture at 1250 °C for 50 h. Residual S contents were analyzed by glow discharge mass spectroscopy (GDMS), sensitive to parts per billion (ppb) levels. APS was performed with standard parameters to yield about 10 mils (250 μm) 8YSZ. Oxidation was performed at 1100 °C for 2000 h or at 1150 °C for 1000 h. Rectangular samples were tested automatically in a vertical tube furnace using 1 h cycles; disk samples were oxidized continuously and manually interrupted only for weight measurements, e.g., every 100 h after 200 h

## 3. Results

### 3.1 Sulfur Effects on TBC Edge Failure

The 1100 °C cyclic oxidation weight change behavior of bare PWA 1484 coupons (solid lines with open symbols), before and after $H_2$ annealing (i.e., at 1.2 and 0.01 ppmw S), is shown in Fig. 1. The as-received material exhibited deviation from adherent behavior at about 300 h, resulting in considerable weight loss (−32 mg/cm$^2$) at the end of the 2000 h test. In contrast, the scale on the $H_2$ annealed sample remained adherent throughout the test, with a final weight gain of only +0.8 mg/cm$^2$. Correspondingly, the visual appearance of the as-received sample exhibited massive interfacial spalling, increased by water immersion after 800 and 2000 h, with little or no spalling visible for the $H_2$ annealed sample, even after immersion. Immersion effects on spallation were previously discussed in more detail.[10] Also shown in Fig. 1 is the behavior for melt-desulfurized PWA 1484, with a S content of ~0.25 ppmw. It too formed adherent scales throughout the test, resulting in a final weight change of +0.8 mg/cm$^2$. Little, if any, improvement was exhibited by $H_2$ annealing a melt-desulfurized sample, producing a final weight change of +0.9 mg/cm$^2$. (The S content of this sample was not analyzed).

The data for the corresponding samples with a TBC of 250 μm of PS-8YSZ is presented as the dashed lines (open symbols). Abrupt (vertical) drops in weight change of 40-60 mg/cm$^2$ usually indicate complete delamination and loss of the TBC from one side of the sample. Lesser amounts correspond to partial spallation of the TBC, usually near an edge. The failure of the TBCs is seen to correlate with the S content of the sample. The first side failure of the TBCs occurred at 200 h for the as-received sample (1.2 ppmw S), partially at 500 h and fully at 900 h for the melt-desulfurized sample (0.25 ppmw S), and at 1200 h for the $H_2$ annealed sample (0.01 ppmw S). The obverse side of each sample failed at 200, 1400, and 2000 h, respectively. (The two TBC faces on the $H_2$ annealed, melt-desulfurized sample failed at 1000 and 1300 h).

A reconstruction of this and auxiliary data is presented in a plot of TBC life as a function of S content in Fig. 2. (Individual data points are presented as small symbols and the averages as large diamonds. $H_2$ annealed, melt-desulfurized data was included in the 0.01 ppmw data even though S was not analyzed.) Despite considerable scatter, there is an identifiable trend toward relatively low lives (<200 h) for S contents ≥1 ppmw and toward relatively high lives (>1000 h) at S levels below ~0.1 ppmw. S levels ≃0.01-0.1 ppmw S represents a practical limit in adhesion behavior according to the adhesion map of Ref 8 and according to the good oxidation behavior in Fig. 1. Therefore, it is not expected that much improvement could occur at lower S contents, even if it were possible to achieve them. At the other extreme, there was a period of time (100-300 h) that the bare 1.2 ppmw S sample exhibited borderline adherent behavior, with a weight gain of ~0.3 mg/cm$^2$, in concert with the corresponding TBC sample weight of about +0.5 mg/cm$^2$ and life of 200 h at these S levels (Fig. 1). Also, the adhesion map indicates transitional/poor behavior at ~1 ppmw S. It can therefore be expected that alloys with >1 ppmw S will exhibit TBC lives

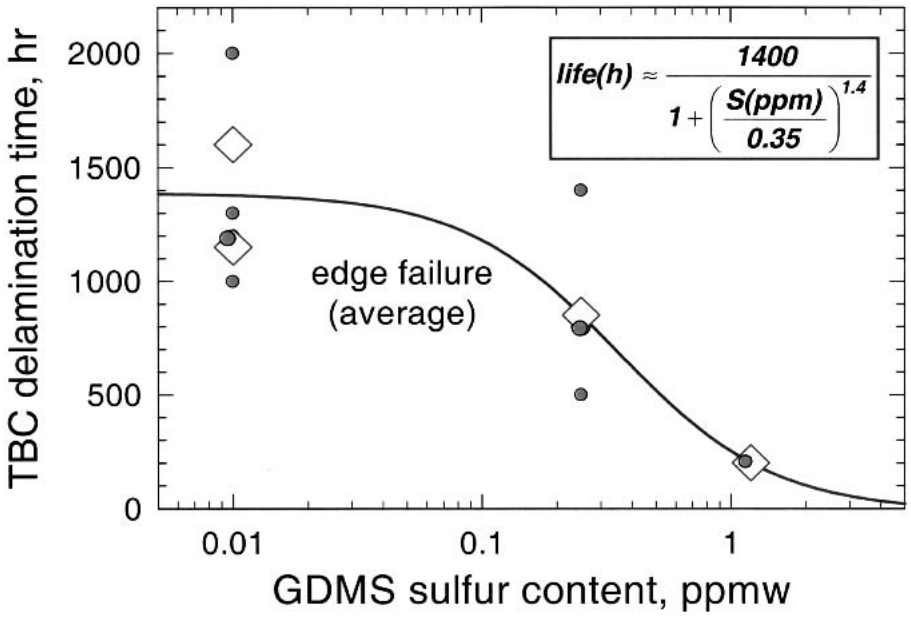


**Fig. 2** Effect of PWA 1484 substrate S content on TBC life in 1100 °C cyclic oxidation tests (small circles, individual coatings; large diamonds, averages)

<200 h. Alternatively, it can be said that the TBC life was increased by 5-10× simply by removing S and preventing its detrimental effects on scale adhesion.

Of course the above correlations of TBC life with substrate oxidation are predicated on the assumption that scale spallation is a primary factor in the TBC spallation mechanism. This notion is widely accepted due to numerous instances where the Pt, Y, Hf, C, and S contents of NiAl bond coats and superalloy substrates have been shown to effect scale adhesion and possibly TBC life.[11-14] In support of this mechanism, the exposed failure surface of the coated PWA 1484 substrate was studied by optical microscopy and scanning electron microscopy (SEM) and found to exhibit a finely dispersed, but considerable, amount of spalling to bare metal for the 1.2 ppmw S sample. The remainder of the surface was a combination of intact oxide area and fractured YSZ areas. Much of the exposed scale was a blue $NiAl_2O_4$ transient spinel oxide, with a healing layer of $Al_2O_3$ underneath this at the metal interface. Presumably, when enough TBC bond area is disrupted by interfacial scale spallation, multiple crack areas link up and produce a critical crack size that results in crack propagation and separation of the TBC layer.[17]

Another aspect of the TBC failure on PWA 1484 is the effect of moisture on delayed failure at room temperature. While some failures occurred immediately upon cool-down, others occurred overnight (desk-top spallation; DTS) or upon water immersion ($H_2O$), in Fig. 1. The former (DTS) occurred on at least one sample side at 200, 800, and 1200 h for the 1.2, 0.25, and 0.01 ppm S samples, respectively. The latter occurred at 2000 h for the 0.01 ppm S sample. These observations reinforce the significance of moisture effects on scale spallation and subsequent TBC failure, as discussed previously.[10,17-19]

Failure initiated predominantly at edges, since the edges were uncoated in these samples. In some cases failure and delamination progressed gradually down the length of the sample, giving an "alligator" appearance.

### 3.2 Segmented Thermal Barrier Coatings

**3.2.1 Grooved or Ribbed Test Patterns.** It appeared that this edge initiation mode could be largely subverted by providing physical impediments to complete delamination. In a first attempt, both ridges and grooves were produced in melt desulfurized (0.25 ppmw S) PWA 1484 substrates to preclude the propagation of a single catastrophic crack. The ridge (or groove) features were about 300 μm (12 mils) in height (or depth) and 250 μm (10 mils) in width. A test pattern network was EDMed into the 1 in. (2.54 cm) diameter disk substrate, yielding a patchwork of segments with dimensions ranging from 1.27 to 5.08 mm (0.050-0.200 in.) on a side.[11] A schematic of the pattern is shown in Fig. 3, with an indexing scheme to identify the segments by their size and position. For example, segment A is 0.050 in. on a side, is the smallest segment, and is closest to the center of the disk. At the other extreme, segment F is the largest at 0.200 in. square, with one corner reaching the periphery of the disc. Segments G, H, and I are special cases in that they are bordered by ridges or grooves on only two or three sides, with a curved periphery being the same as on flat, non-segmented samples.

The cyclic weight change behavior of four segmented disk samples is shown in Fig. 4. Both ribbed (ridges) and grooved samples were tested in 1100 °C interrupted oxidation tests, in the as-sprayed condition or after subsequent hydrogen annealing (1250 °C for 50 h). (These data were corrected for backside, non-segmented TBC failure at the points indicated by arrows). The weight change of the ribbed samples shows very little weight loss, if any, indicating that the ribbed segments prevented TBC spallation out to 2000 h. (Some TBC was lost over the ribs themselves but none within the inscribed segment area.) The

grooved samples, however, exhibited incremental weight losses throughout the test whenever a portion of the TBC, corresponding to one segment, became fully detached. Nonetheless, a considerable number of the smaller, inner segments on the grooved sample remained intact after 2000 h (Fig. 5). This figure also shows the relatively intact TBC for all segment sizes on the ribbed sample.

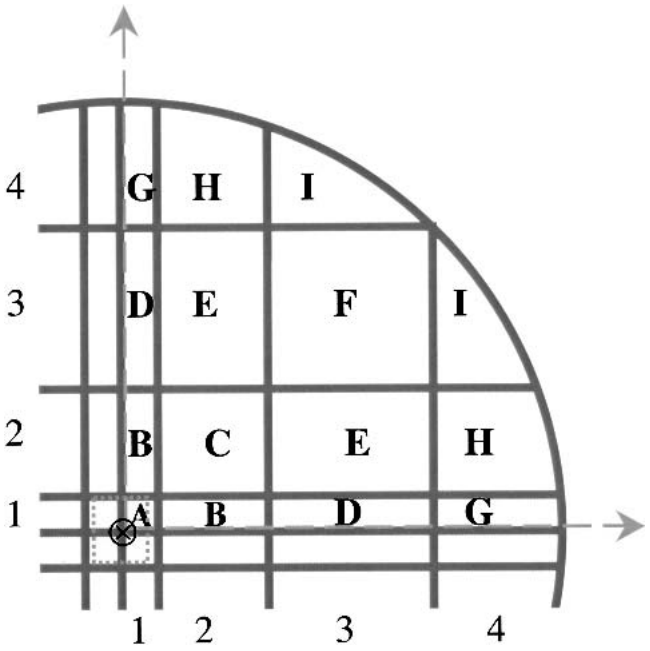


**Fig. 3** EDM test pattern grid of grooves or ribs in substrate to produce segmented TBC, showing indexing scheme. (Quarter round sector of 1 in. diameter disk sample)

The spallation trend for the grooved sample is shown in a more quantitative manner by plotting the TBC segment spallation time as a function of the relative area (and position) in Fig. 6. Here the smallest inner segment A is used as the reference segment. As the size is increased, the life was reduced from >2000 h to 1000-1300 h. Only the F and I-type segments failed universally; the other types had at least one equivalent segment survive 2000 h. Little effect is noted for the hydrogen annealing treatment. The segments that abut the free edge of the disc (G, H, and I) exhibit somewhat reduced lifetime, though still generally improved from the base lifetime values (300-400 h) produced for the flat backsides of these and similar samples.

It is clear from the above experiment that grooved segment boundaries produce TBC lives in excess of 2000 h for segments 0.100 in. (2.5 mm) on one side or below. Similarly, and even more remarkable, ribbed TBC segments exhibit an apparent immunity to oxidation-induced delamination, at least for dimensions of 5.1 mm (0.200 in.) square or below. A further advantage of the ribbed segments over the grooved ones might be that the grooves could serve as stress concentrations in the substrate material and shorten the thermal fatigue life of the component. A disadvantage of the ribbed structure is the lack of thermal insulation over exposed ribs (if produced flush with the TBC segment surface) or the non-aerodynamic disruptions caused (if the ribs are also coated, as in Fig. 5a).

**3.2.2 Enlarged Rib Patterns.** To more fully demonstrate the limitations of the ribbed structure and to optimize the amount of ribs, a new set of samples were produced with increased segment sizes. Specifically, 1 in. diameter disks of melt-desulfurized PWA 1484 were EDMed with either 0.09, 0.18,

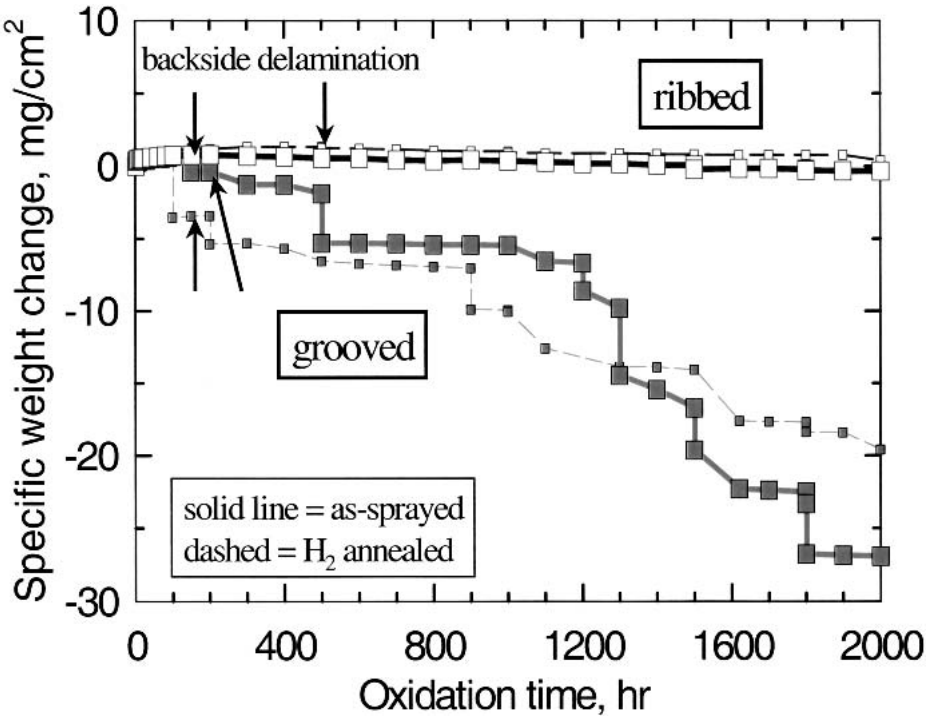


**Fig. 4** Comparative weight change behavior of ribbed and grooved segmented 10 mil (250 μm) TBCs on PWA 1484 (1100 °C interrupted oxidation)

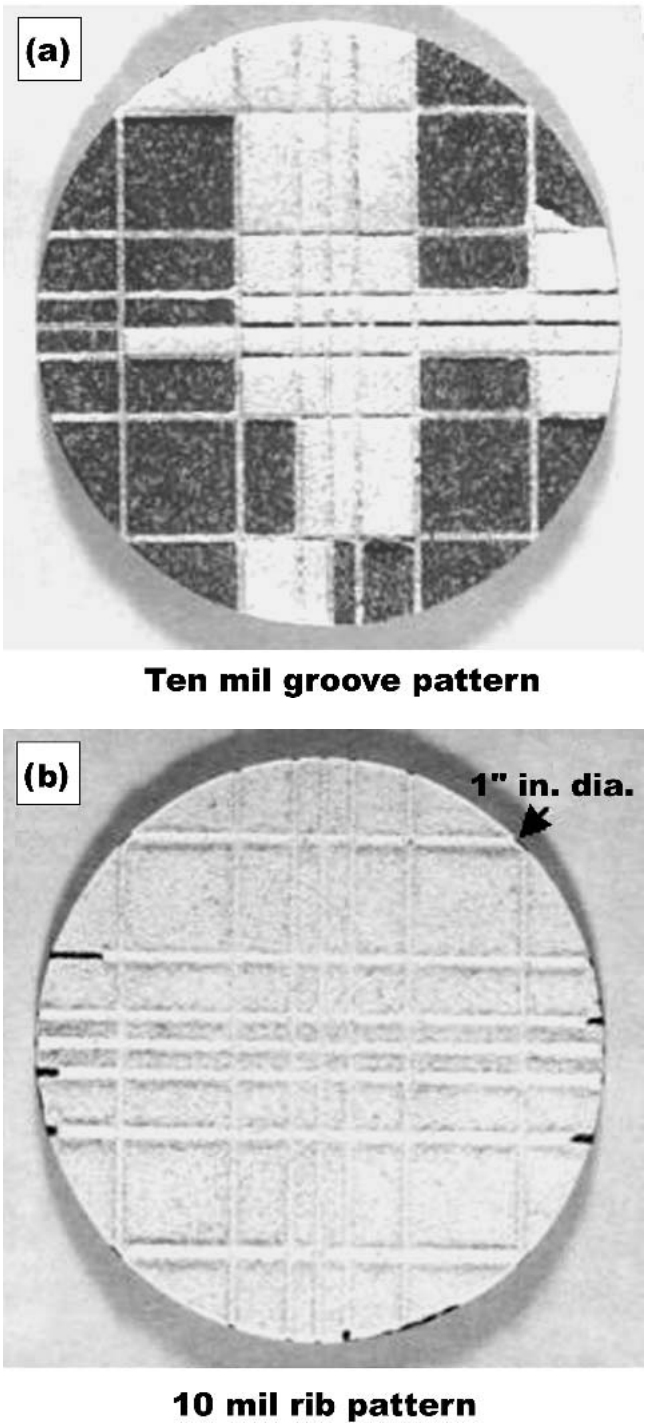


**Fig. 5** Appearance of segmented TBC on 1 in. (2.54 cm) dia. PWA 1484 discs after 2000 hr interrupted oxidation at 1100 °C: **(a)** grooved and **(b)** ribbed

0.35, and 0.71 in. square segments (0.225, 0.45, 0.90, 1.80 cm), having 64, 16, 4, or 1 segment for interrupted oxidation at 1100 and 1150 °C. Alternately, 0.50 × 0.75 in. rectangular samples (1.27 × 1.9 cm) were machined with 0.125 and 0.25 in. (0.32, 0.64 cm) segments, or a single peripheral ridge producing 24, 6, or 1 segment tested in 1 h cyclic oxidation tests.

The weight change behavior of these samples was not very informative, as with the previous ribbed samples, because failure was not generally associated with TBC spallation, except for the flat backsides. Rather, the failure mode observed was a circular buckling at the middle of a segment. Examples of this failure mode, in interrupted (primarily 100 h cycles) and cyclic (1 h cycles) oxidation tests at 1100 °C, are shown in Fig. 7 and 8. The interrupted oxidation disk samples show massive buckling failure at 1000 h for the largest, inscribed, 18 mm (0.71 in.), single-segment sample and at 1400 h for the sample with four segments at half the size at 9 mm (0.35 in.). No buckling was observed up to 2000 h for samples with 16 or 64 segments ≤4.5 mm (0.18 in.) on a side. Similarly, the rectangular cyclic oxidation coupon with the largest, inscribed, 12.7 × 19 mm (0.5 × 0.75 in.), single segment failed at 2000 h, with no failure observed for samples with 6 or 24 segments ≤6.4 mm (0.25 in.) on a side.

The buckling life data is displayed along with similar 1150 °C results in Fig. 9. Here the format adopted is similar to that of a fatigue plot in that life (and runout, arrows) is displayed on the horizontal axis and a parameter associated with decreasing failure resistance (segment size) is the vertical axis. Data points labeled E refer to the average edge failure lives of the corresponding flat backsides of the segmented samples.

Edge failures universally exhibit the lowest life of all the segments in that test series. The data at 1150 °C is similar to that obtained at 1100 °C, except that the magnitude is reduced by a factor of 3-5. Also the data for interrupted tests, with final cycle duration of 100 h, did not generally exhibit lives greater than samples tested with 1-h cycle durations. This suggests that total oxidation exposure time is the critical factor controlling failure in these tests, provided some minimum amount of cycling is experienced.

## 4. Discussion

Reducing the S content of the substrate was helpful in extending the oxidative failure time of plasma sprayed TBCs without a bond coat. Nevertheless, the failure mode remained just as distinctive in that edge-initiated delamination still proceeded rapidly over the entire surface. Such failure could indicate weak bonding across the mixed TBC, $NiAl_2O_4/Al_2O_3$, bare metal fracture interface. It may also reflect an aggregate thermal stress effect of the entire TBC layer upon the free edge.

### *4.1 Grooved Segments*

In this regard, an analytical expression has been developed, predicting a maximum in the interfacial shear stress at the free edge of an oxide-metal couple.[20] This result was also obtained by finite element analyses of TBC-coated superalloys.[21] Both treatments find a reduction in this maximum with decreasing lateral dimensions of the bi-plate system, consistent with the increased lives for smaller grooved segments. Reduced interfacial shear stress at free edges is consistent with the increased lifetimes of the smaller grooved segments in the current study. Strictly speaking, the segments do not have free edges in that the plasma sprayed coating penetrates the grooves as well, providing a continuous, but non-planar, overall coating. With continuing exposure and cycling, however, these grooves became fracture sites and one by one initiated delamination of the adjacent segments.

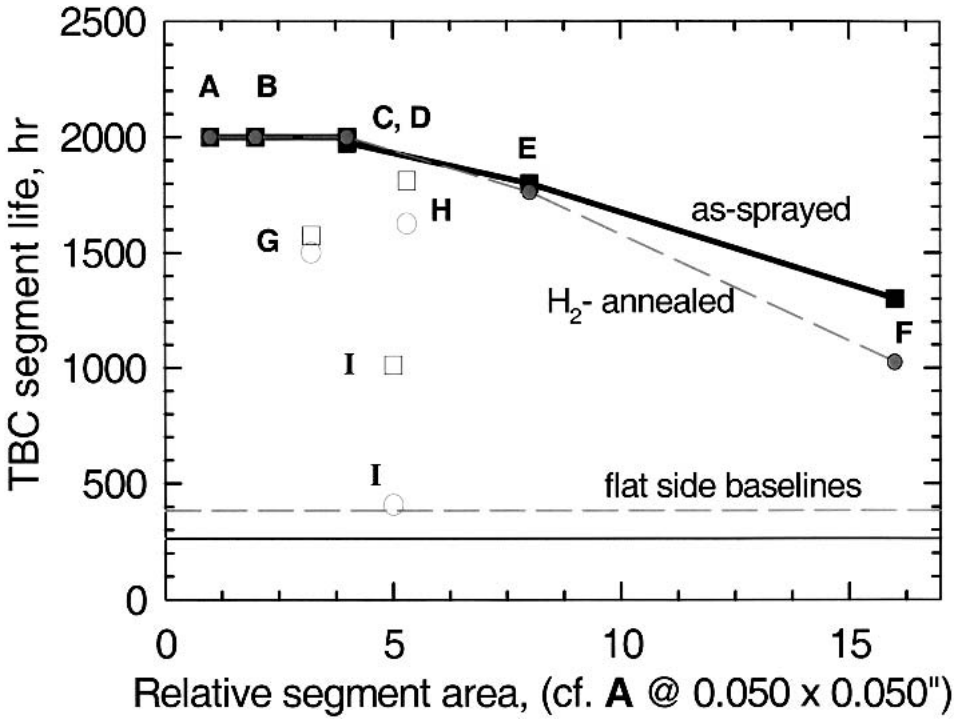


**Fig. 6** Effect of grooved segment size on TBC spallation life as compared with flat backside spallation

Other studies report increased thermal shock and interfacial spalling resistance for TBCs that have been segmented by surface cracking (from tensile stresses achieved by YSZ sintering, then cooling, both while under thermal gradients).[22] Up to 30 cracks per inch (spaced 0.85 mm) were found to increase the surface temperature capability of a TBC without an interface crack. This is consistent with the maximum lives produced for the smallest grooved segments, i.e., 1.27 mm, in the current study.

It is acknowledged that numerous other references to segmented TBCs exist, but due to vast differences in scale, they are considered to have only indirect relevance to the present mechanism, as cited previously in Ref 16. For example, the finely spaced cracks in PVD TBCs are the most widely recognized "segmented" strain tolerant structure. However, their spacing is on the order of micrometers, whereas the current structure is based on millimeter-sized elements. Similarly, the textured surface provided by laser grooving is on the scale of micrometers, both in depth and in spacing. At the other extreme, very large 10-250 cm (0.4-10 in.) wide segments were produced by a machined grid of slots in the TBC to reduce long-range stresses, primarily for thick TBCs. While this structure may benefit from the same mechanisms operative in the present architectures, it is apparent that the specified dimensions (2.5 cm) are much greater than the optimums found in the current study. Furthermore, much of the range specified would not be practical for many turbine components in the 5-10 cm size range, whereas the 2-5 mm spaced network proposed here appears more reasonable.

### 4.2 Ribbed Segments

For the ribbed segments, the free edge was totally eliminated by providing a "wall" bounding the periphery of each segment. This caused a transition to a buckling-type failure, described by the equation for the biaxial stress σ on an edge-clamped plate of thickness $h$ and buckle radius $r$ as noted for example in Ref 23:

$$\sigma_b = \frac{1.22\,E_{TBC}}{1-\nu^2_{TBC}}\left(\frac{h_{TBC}}{r_b}\right)^2 \quad \text{(Eq 1)}$$

Thus, the critical stress for buckling is controlled by a geometric parameter $(h/r)^2$, where $h$ is the thickness of the TBC and $r$ is the radius of the delaminated area subject to buckling. A schematic representation of one buckled segment is shown in Fig. 10. In decreasing the buckle dimensions by providing a physical barrier, i.e., $2r_b \approx$ rib spacing, the critical stress required for buckling is seen to increase.

The origin of the stress is the thermal expansion mismatch stress between TBC and substrate. It has been defined by the equation for a composite laminate subject to a change in temperature[18]:

$$\sigma_{cte} = \frac{(\Delta\alpha_{cte}\Delta T)E_{TBC}}{(1+R)(1-\nu_{TBC})} \quad \text{(Eq 2)}$$

where $R$ is given by

$$R = \frac{h_{TBC}E_{TBC}\,(1-\nu_{TBC})}{h_m E_m\,(1-\nu_m)} \quad \text{(Eq 3)}$$

For the equations above, $\nu_m = 0.33$, $\nu_{TBC} = 0.25$, $E_{1484} = 210$ MPa, and $E_{TBC} = 27.6$ GPa are assumed, although $E_{TBC}$ may approach 100 GPa upon densification.[21] Also $\alpha_{TBC} = 10.8 \times 10^{-6}$/ °C, and $\alpha_m = 16.2$ and $16.6 \times 10^{-6}$/°C at 1100 and 1150 °C,

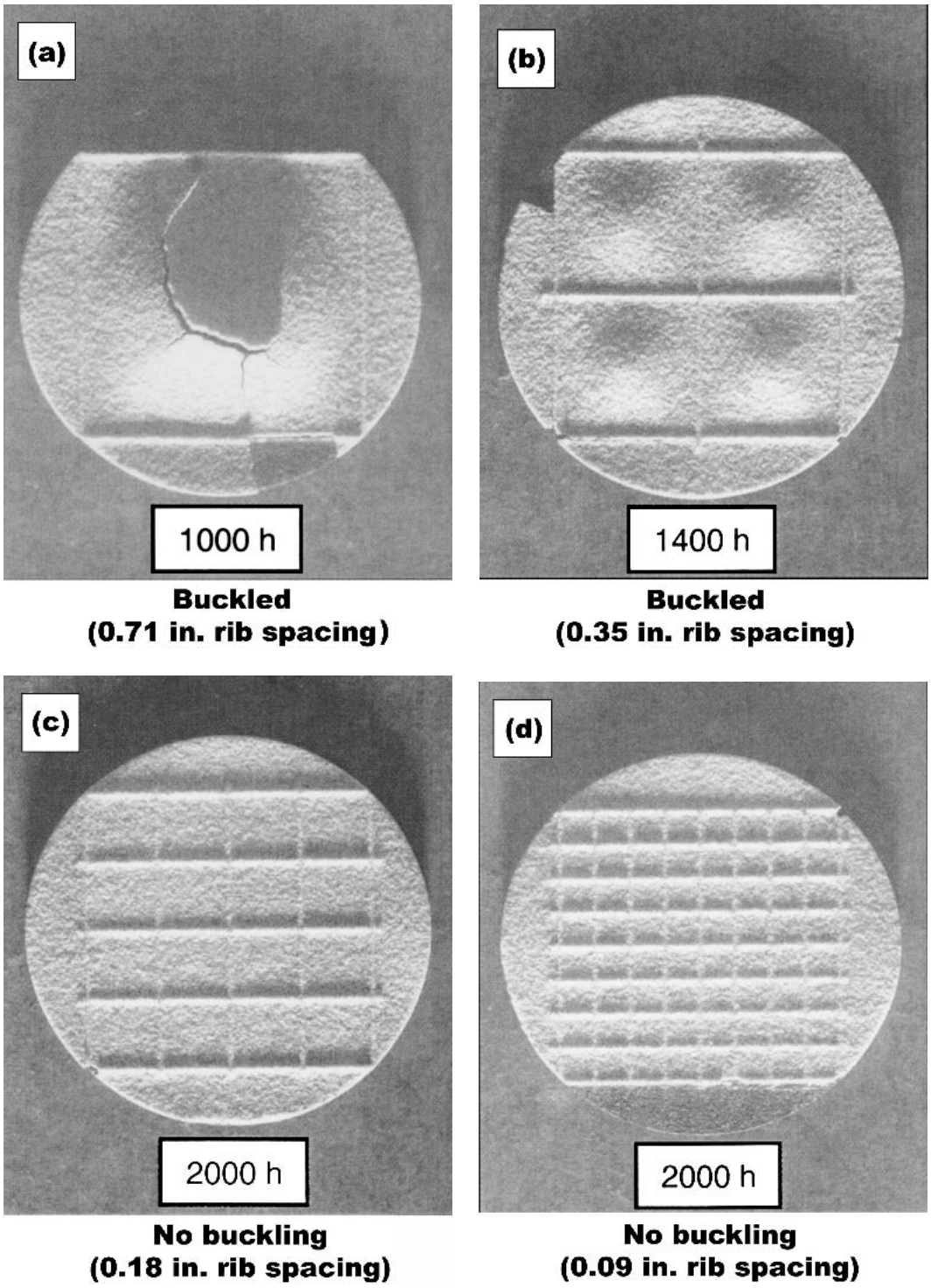


**Fig. 7** Surface appearance of ribbed segment disc samples (1 in. diameter) after interrupted (100 h cycles) oxidation at 1100 °C for 1000, 1400, 2000, and 2000 h (10 mil PS 8YSZ on PWA 1484)

respectively. $R$ was thus determined to be 0.0736 for a 250 μm (10 mil) coating ($h_{TBC}$) on a 1 mm (40 mil) substrate thickness ($2h_M$).

By requiring that $\sigma_{cte} > \sigma_b$ and combining Eq 1-3, an expression for a critical buckling diameter, $2r_b^*$, can be derived. Below this value, buckling caused by thermal expansion mismatch stresses would not be expected to occur. These values are shown as horizontal lines in Fig. 9, and represent critical segment spacings (buckle diameters) for the two test temperatures. In accord with this prediction, note that the experimental data below these

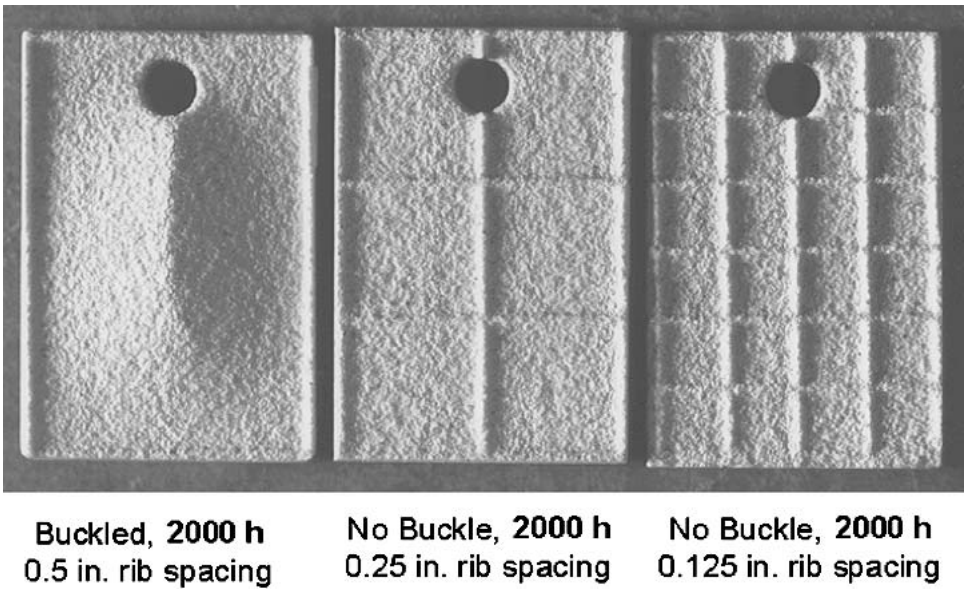


**Fig. 8** Surface appearance of ribbed segment rectangular samples (0.5 × 0.75 in.) after cyclic (1 h cycles) oxidation at 1100 °C for 2000 h (10 mil PS 8YSZ on PWA 1484)

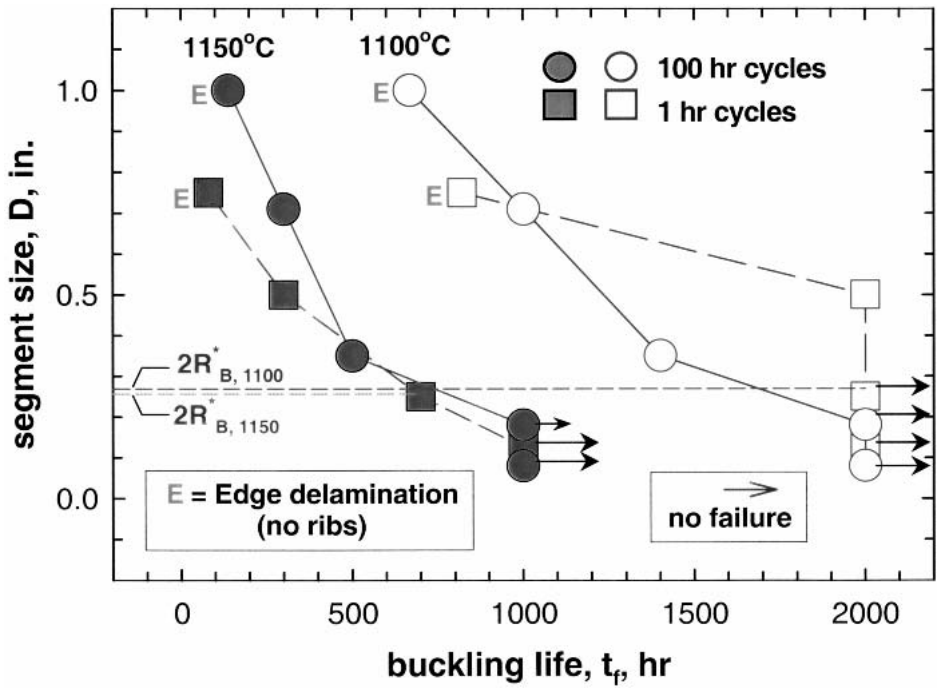


**Fig. 9** Effect of segment size and test temperature on buckling life for segmented TBCs in interrupted and cyclic exposures (Points labeled "E" refer to edge delaminations of non-segmented backside or control samples; arrows indicate no failure at end of test)

lines indicate no failure and suggest an indefinite runout, or thermal fatigue limit to buckling failure. (One data point below the line may be at the borderline of observable failure, i.e., the short arrow applying to the interrupted disk sample with sixteen 0.18 in. segments, oxidized at 1150 °C). Buckling was not apparent from examination of this sample under oblique lighting. Some detachment was only marginally evident for a few segments at 1000 h by measuring thickness differences between the segment centers and corners with pointed micrometers.)

While the concepts of a critical buckling stress and radius appear useful, they alone cannot explain the strong effect of test temperature. The difference in predicted buckling stress for the two test temperatures, between $\sigma^*_{b,\ 1100}$ and $\sigma^*_{b,\ 1150}$, appears minor; however, the failure times are greatly reduced at the

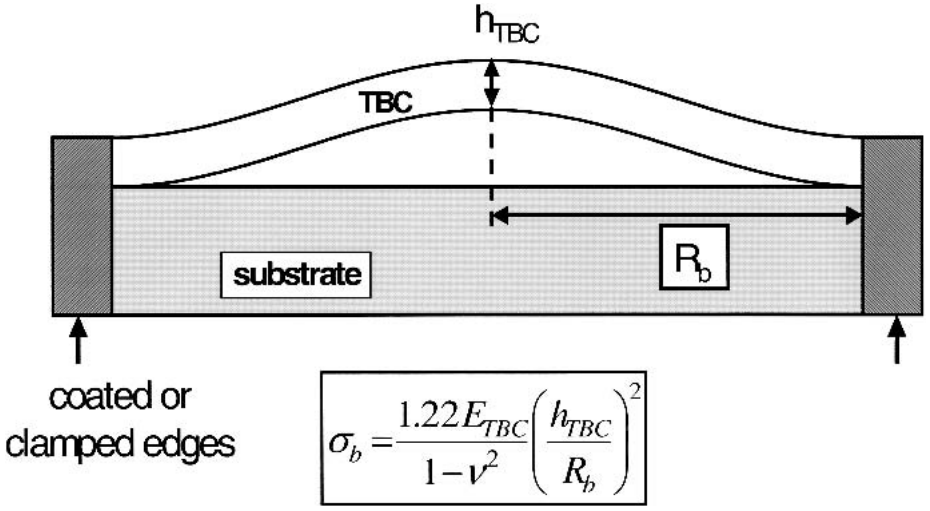


**Fig. 10** Schematic of TBC buckling within a defined segment (constrained edges), such as produced by ribs

higher temperature. Presumably, the greater damage caused by increased scale thickness and spallation is operative here, in accord with current TBC failure conventions.

The critical buckling stress in Eq 1 applies to unbonded plates and thus assumes that full delamination had taken place. Certainly TBC or scale detachment did not exist initially. Rather, the interface may have deteriorated gradually and was only completed during the actual buckling process, when the strain energy release rate exceeds the interfacial energy formed during final fracture. Therefore the critical buckling stress $\sigma_b$* can be considered only as a lower limit for a fully separated TBC. For partially bonded interfaces, it must be raised by an amount commensurate with the relative amount of bonded area.

For the purposes of this discussion, it is also assumed that the laminates are stress-free at the test temperature. Creep and sintering effects on the projected thermal stresses causing failure are neglected. The edge failures (*E*) of non-segmented samples are subject to a different failure criteria and do not directly verify these predictions, but are included to show a relative (base) TBC life in that failure mode. It has been stated that the critical stress to cause buckling of a cracked laminate element (i.e., one unconstrained end) is 1/4 $\sigma_b$*.[24] This is consistent with the greatly reduced time of failure and lack of durability for flat substrates exhibiting edge failure.

No other studies are known to have used a network of substrate or bond coat ribs to produce TBC segmentation. The ribbed structures are shown here to be more resilient than grooved substrates regarding TBC delamination and spalling. Optimization of the rib spacing, height, and geometry to a design that is practical for turbine component surfaces may improve upon premature massive TBC delamination in cyclic oxidation exposures. This must be accomplished without seriously compromising aerodynamic performance, thermal leakage through the ribs, added weight, or notch effects. Given that the height and width of the present configurations were only on the order of the coating thickness and could be spaced as wide as 5 mm, some combinations are likely to be effective without incurring serious penalty. It is suggested that the ribbed TBC architecture may offer benefits to TBC systems in general, including PVD ceramic top coats with aluminide or MCrAlY bond coats.

## 5. Summary

This study has shown that considerable oxidative durability can be obtained for plasma-sprayed 8YSZ TBCs on single-crystal superalloys without a bond coat. Reductions in the PWA 1484 substrate S impurity level to below 0.1 ppmw improve scale adhesion and allows 1100 °C cyclic oxidation lives on the order of 1000-1500 h. Failure occurred by massive, complete edge delamination of the coating. Segmenting the thermal barrier, through a network of grooves or ribs produced in melt desulfurized PWA 1484 substrates by EDM, further improved no bond coat TBC life. Grooved samples allowed segments smaller than 0.1 in. (2.5 mm) wide to survive 2000 h in 1100 °C interrupted (100 h cycle) oxidation tests. Ribbed segments smaller than 0.25 in. (6.35 mm) wide also survived, while larger ones failed by buckling at times inversely related to the segment size. Survival was consistent with critical buckling stresses predicted for laminate plates subjected to biaxial thermal expansion mismatch stresses. Higher temperature decreased lifetime considerably, but more rapid cycling did not. It is suggested that the ribbed TBC architecture may offer benefits to generalized TBC systems, including PVD ceramic top coats with aluminide or MCrAlY bond coats.

### Acknowledgments

The author is grateful to D. Zhu for helpful discussions, D. Humphrey for performing hydrogen annealing, G. Leissler for plasma spraying, and L. Graham (PCC) for supplying all PWA 1484 castings.

### References

1. R.A. Miller and J.K. Doychak: "Plasma Sprayed Ceramic Thermal Barrier Coating for NiAl-based Intermetallic Alloys," US Patent 5,302,465, April 12, 1994.
2. J.C. Schaeffer, W.H. Murphy, W.B. Connor, B.A. Nagaraj, and H.B. Vakil: "Thermal Barrier Coating System Having No Bond Coat," US Patent 5,538,796, July 23, 1996.
3. A.M. Freborg, B.L. Ferguson, W.J. Brindley, and G.J. Petrus: "Model-

ing Oxidation Induced Stresses in Thermal Barrier Coatings," *Mater. Sci. Eng.,* 1998, *A245,* pp. 182-90.
4. M.Y. He, A.G. Evans, and J.W. Hutchinson: "The Ratcheting of Compressed Thermally Grown Thin Films on Ductile Substrates," *Acta Mater.,* 2000, *48,* pp. 2593-601.
5. G.H. Meier, F.S. Pettit, and J.L. Smialek: "The Effects of Reactive Element Additions and Sulfur Removal on the Adherence of Alumina to Ni- and Fe-Base Alloys," *Werkstoffe Korrosion,* 1995, *46,* pp. 232-40.
6. J.L. Smialek: "Maintaining Adhesion of Protective $Al_2O_3$ Scales," *JOM,* 2000, *52*(1), pp. 22-26.
7. J.L. Smialek: "Advances in the Oxidation Resistance of High-Temperature Turbine Materials," *Surf. Interface Anal.,* 2001, *31,* pp. 582-92.
8. J.L. Smialek: "Toward Optimum Scale and TBC Adhesion on Single Crystal Superalloys" in *High Temperature Corrosion and Materials Chemistry, 98-9,* E.J. Opila, P.Y. Hou, D.Shores, M. McNallan, and R. Oltra, ed., The Electrochemical Society, Pennington, NJ, 1998, pp. 211-20.
9. J.L. Smialek and B.A. Pint: "Optimizing Scale Adhesion for Single Crystal Superalloys," *Mater. Sci. Forum,* 2001, *369-372,* pp. 459-66.
10. J.L. Smialek and G.N. Morscher: "Delayed Alumina Scale Spallation on Rene'N5: Moisture Effects and Acoustic Emission," *Mater. Sci. Eng, A,* 2002, *332*(1-2), pp. 11-24.
11. J.A. Haynes, B.A. Pint, K.L. Moore, I.G. Wright, and J.L. Smialek: "Superalloy Substrate Influences on the Oxidation Behavior of Aluminide Bond Coatings" in *John Stringer Symposium on High Temperature Corrosion,* P.F. Tortorelli, I.G. Wright, and P.Y. Hou, ed., ASM International, Materials Park, OH, 2002, in press.
12. I.G. Wright, B.A. Pint, W.Y. Lee, K.B. Alexander, and K. Prüβner: "Some Effects of Metallic Substrate Composition on Degradation of Thermal Barrier Coatings" in *High Temperature Surface Engineering,* Book 693, J. Nicholls and D. Rickerby, ed., Institute of Materials, London, UK, 2000, pp. 95-113.
13. W.Y. Lee, Y. Zhang, I.G. Wright, B.A. Pint, and P.K. Liaw: "Effect of Sulfur Impurity on the Scale Adhesion Behavior of a Desulfurized Ni-based Superalloy Aluminized by Chemical Vapor Deposition," Metall. Trans., *29A,* pp. 833-41 (1998).
14. B.A. Pint, I.G. Wright, W.Y. Lee, Y. Zhang, K. Prüβner, and K.B. Alexander: "Substrate and Bond Coat Compositions: Factors Affecting Alumina Scale Adhesion," *Mater. Sci. Eng.,* 1998, *A245,* pp. 201-11.
15. J.L. Smialek: "Scale Adhesion, Sulfur Content, and TBC Failure on Single Crystal Superalloys," *Ceram. Eng. Sci. Proc.,* 2002, *23*(4), pp. 485-95.
16. J.L. Smialek, "Segmented Thermal Barrier Coating," U.S. Patent 6,316,078, Nov. 13, 2001.
17. X. Peng and D.R.Clarke: "Piezospectroscopic Analysis of Interface Debonding in Thermal Barrier Coatings," *J. Am. Ceram. Soc.,* 2000, *83*(5), pp. 1165-70.
18. V. Sergo and D.R. Clarke: "Observation of Subcritical Spall Propagation of a Thermal Barrier Coating," *J. Am. Ceram. Soc.,* 1998, *81*(12), pp. 3237-42.
19. R. Janakiraman, G.H. Meier, and F.S. Pettit: "The Effect of Water Vapor on the Oxidation of Alloys that Develop Alumina Scales for Protection" in *Cyclic Oxidation of High Temperature Materials,* M. Schutze and W.J. Quadakkers, ed., European Federation of Corrosion, Institute of Materials, London, UK, 1999, pp. 38-62.
20. J.K. Tien and J.M. Davidson: "Oxide Spallation Mechanisms" in *Stress Effects and the Oxidation of Metals,* J.V. Cathcart, ed., AIME, New York, 1975, pp. 200-19.
21. D. Zhu, L.J. Ghosn, and R.A. Miller: "Effect of Layer-Graded Bond Coats on Edge Stress Concentration and Oxidation Behavior of Thermal Barrier Coatings" in *High Temperature Materials Chemistry, 98-9,* P.Y. Hou, M.J. McNallan, R. Oltra, E.J. Opila, ed., Electrochemical Society, Pennington, NJ, 1998, pp. 170-89 (also NASA TM 1998-208505, Washington, DC, 1998).
22. K. Kokini, A. Banerjee, and T.A. Taylor: "Thermal Fracture of Interfaces in Precracked Thermal Barrier Coatings," *Mater. Sci. Eng.,* 2002, *A323,* pp. 70-82.
23. H.E. Evans, G.P. Mitchell, R.C. Lobb, and D.R.J. Owen: "A Numerical Analysis of Oxide Spallation," *Proc. R. Soc. London,* 1993, *440A,* pp. 1-22.
24. M.D. Thouless: "Combined Spalling and Cracking of Films," *J. Am. Ceram. Soc.,* 1993, *76,* pp. 2936-38.